Black-Box Identification for PLC based MPC of a Binary Distillation Column

B. Huyck [*,**,***] **F. Logist** [**] **J. De Brabanter** [*,***]
J. Van Impe [**] **B. De Moor** [***]

[*] *Department of Industrial Engineering, KaHo Sint Lieven, Gent, Belgium (e-mail: Bart.huyck@esat.kuleuven.be)*
[**] *Department of Chemical Engineering (CIT - BioTeC), K.U.Leuven, Leuven, Belgium*
[***] *Department of Electrical Engineering (ESAT - SCD), K.U.Leuven, Leuven, Belgium*

System identification; Linear MIMO; Chemical Industry; Distillation columns; Automatic Process Control;

Abstract: This paper describes the identification of a binary distillation column in view of introducing an MPC system. Since the intension is to exploit only Programmable Logic Controllers (PLCs), which are commonly used in practice but have a limited computational power, accurate but also simple (linear) models have to be constructed. Hereto, several types of linear black-box MIMO models (i.e., ARX, ARMAX, output error) are identified and reduced based on a Hankel Singular Value decomposition. Models are derived for two data sampling rates, one with 5 s and one with 60 s. It has been observed that (*i*) only ARX and ARMAX models are able to predict the column's behavior accurately and that (*ii* the best prediction in validation is obtained for the ARMAX models.

1. INTRODUCTION

In a world where economic and environmental issues become more and more important, efficient control systems have become indispensable. When dealing with complex processes, Model Predictive Control (MPC) is one of the possible control strategies. According to Piche et al. [2000] more than 2000 MPC controllers are used in industry. Most of these industrial MPC applications use linear empirical models [Qin and Badgwell, 2003]. In practice, current linear and non-linear MPC algorithms require powerful computers. However, since Programmable Logic Controllers (PLCs) with less computational power are used a lot in industry for control, it might be interesting to explore the possibilities and limitations of these devices for MPC. As an industrial example, a pilot scale binary distillation column, is selected. The column is currently controlled by PI controllers, but the goal is to upgrade the control system with a linear MPC running on a PLC. However, before a model based controller can be used on a PLC, an accurate (but simple) process model has to be constructed. Hence, the aim of this paper is to derive a black-box Multiple Input Multiple Output (MIMO) model for the column, but we limit ourself to linear parametric models (e.g., ARX, ARMAX, and output error).

The paper is structured as follows. Section 2 describes the binary distillation column. Section 3 presents the identification procedure covering data collection and preparation, model selection and validation. The resulting identified models and the validation results are reported in Section 4. Finally, Section 5 summarises the main conclusions.

2. DISTILLATION COLUMN SET-UP

The experimental set-up involves a computer controlled packed distillation column (see Figures 1 and 2). The column is about 6 m high and has an internal diameter of 6 cm. The column works under atmospheric conditions and contains three sections of about 1.5 m with Sulzer CY packing (Sulzer, Winterthur) responsible for the separation. This packing has a contact surface of 700 m^2/m^3 and each meter packing is equivalent to 3 theoretical trays. The feed stream containing a mixture of methanol and isopropanol is introduced into the column between the packed sections 2 and 3. The temperature of the feed can be adjusted by an electric heater of maximum 250 W. At the bottom of the column a reboiler is present containing two electric heaters of maximum 3000 W each. In the reboiler, a part of the liquid is vaporised while the rest is extracted as bottom stream. At the column top a total condensor allows to condense the entire overhead vapour stream, which is then collected in a reflux drum. A part of the condensed liquid is fed back to column as reflux, while the remainder leaves the column as the distillate stream.

In this set-up the following four variables can be manipulated: the reboiler duty Qr (W), the feed rate Fv (g/min), the duty of the feed heater Qv (W) and the distillate flow rate Fd (g/min). Measurements are available for the distillate flow rate Fd (g/min), the feed flow rate Fv (g/min) and nine temperatures, i.e., the temperature at the top of the column Tt (°C), the temperatures in the center of every packing section ($Ts1$ (°C), $Ts2$ (°C) and $Ts3$ (°C), respectively), the temperature between section 1

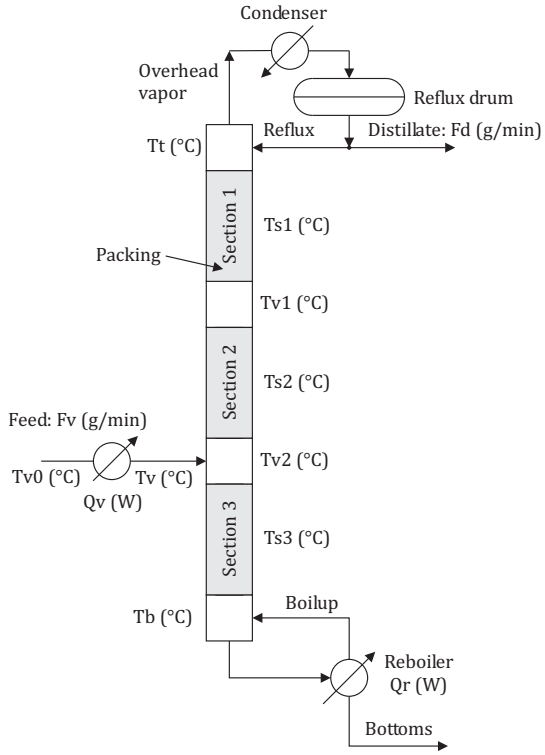

Fig. 1. Diagram of the pilot scale distillation column.

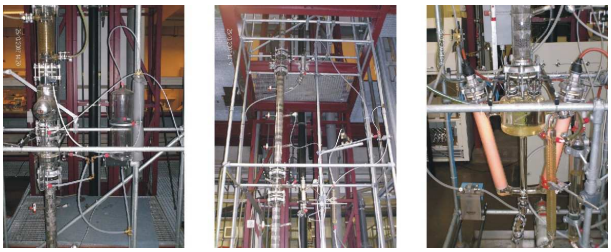

Fig. 2. Pictures of the pilot scale distillation column: condenser (left), packed section and feed introduction (centre), and reboiler (right).

and 2 $Tv1$ (°C), the temperature between section 2 and 3 $Tv2$ (°C), the temperature in the reboiler of the column Tb (°C), and the temperatures of the feed before and after heating ($Tv0$ (°C) and Tv (°C), respectively). All actuators and sensors are connected to a Compact Fieldpoint (National Instruments, Austin) with a controller interface cFP-2100 and I/O modules cFP-AIO-610 and cFP-AI-110. A Labview (National Instruments, Austin) program is developed to control the actuators and to register the variables. There is no online measurement of the concentrations in the distillate and bottom stream, but they can be inferred from the temperatures.

3. MODEL IDENTIFICATION

For linear MPC, a linear model is required. Therefore, a parametric model is fitted following the Box-Jenkins modelling procedure. In order to construct the model following steps are performed: (*i*) Experiment, (*ii*) Data preparation, (*iii*) Model selection and Parameter estimation, and (*iv*) Validation. The processing is performed using the Matlab System Identification Toolbox [Ljung, 2008].

3.1 Experiment

Before the experiment is started, the column is kept for two hours at a constant operating point to ensure the column is in steady state. The nominal steady state values of the different manipulated variables are: a distillate flow rate Fd of 70 g/min, a feed flow rate Fv of 150 g/min, a feed heater duty Qv to maintain a feed temperature Tv of 40 °C and a reboiler power Qr of 4400 W. These nominal values are known to yield an appropriate operating point for the column. When the column has reached steady state, Pseudo Random Binary Noise (PRBN) test signals are applied. These PRBN test signals are passed either to the setpoints of the different PI controllers in the system or directly to the manipulated variables as shown on the schematic overview of the column's loops and measuring points in Figure 3.

When the PRBN signals are applied, all manipulated variables switch between 2 values. The distillate flow rate Fd varies between 60 and 80 g/min, the feed flow rate Fv changes between 120 and 180 g/min, the feed heater duty Qv is manipulated to obtain feed temperatures Tv of 35 and 45 °C, and the reboiler power Qr switches between 3900 and 4900 W. The ambient temperature cannot be manipulated and is considered as a disturbance input of the system. The data are recorded with a sample period of 20 ms, which is also the time between two program loops of the Labview program controlling the column.

The outputs of the system are five temperatures along the column, i.e., the top temperature Tt, the temperature in the middle of the first $Ts1$, second $Ts2$ and third packing $Ts3$ and the bottom temperature Tb.

3.2 Data preparation

The original dataset, which is recorded at the same rate as the control of the column, i.e., 50 Hz, is reduced to a dataset with a sampling period of 5 s (*dataset A*), and a dataset with a sampling period of 60 s (*dataset B*). This reduction is done by simply taking the recorded value every 5 or 60 s without averaging or (pre)filtering. In literature, e.g., in Qin and Badgwell [2003], is indicated that MPC algorithms work with interval times of one minute or higher, so the model extracted from dataset B will probably be used. However, if technically possible, the model from dataset A with a sampling interval of 5 s will be employed. Before the identification process is started, the data are detrended and normalised. Finally, the recorded data are split into two parts: the first 2/3 are used to identify the model and will be referred to as *dataset X1*, while the rest is exploited for validation and will be referred to as *dataset X2*, where X is A or B.

3.3 Model selection and parameter estimation

The aim is to construct linear MIMO black-box models for the distillation column. Hereto, different polynomial models are tried, e.g., ARX, ARMAX, and output error (OE), which can all be represented for n_u control variables and n_y output variables by the following general formulation [Ljung, 2008]:

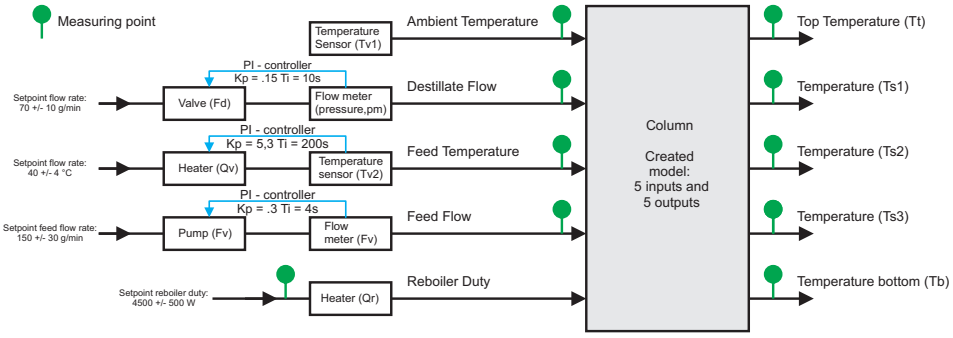

Fig. 3. Diagram of the column's control loops (i.e., three PI-controllers) and measuring points.

$$A(q)y(t) = \sum_{i=1}^{n_u} \frac{B_i(q)}{F_i(q)} u_i(t - n_{k_i}) + \frac{C(q)}{D(q)} e(t). \quad (1)$$

Here, $A(q)$, $B_i(q)$, $C(q)$, $D(q)$ and $F_i(q)$ are matrix polynomial expressions in the shift operator q^{-1} which shifts samples back in time. The order of the polynomial expressions is indicated by respectively n_a, n_b, n_c, n_d and n_f. n_k introduces for the control an additional shift back in time in order to incorporate system delays. For the MIMO ARX model, only the matrix polynomial expressions $A(q)$ and $B_i(q)$ have to be fitted in Equation (1).

To identify a MIMO ARX model for dataset A1, models are constructed with different values for parameters n_a, n_b, and n_k. n_a and n_b are allowed to change from 1 to 25, n_k is fixed and set equal to 1 due to the fact that some variables change faster than the sample period of 5 s. For dataset B1, the parameters n_a and n_b are adapted between 1 and 20 while n_k is set again equal to 1. Higher values for n_k lead to less accurate models for both datasets.

For ARMAX models, polynomials $A(q)$, $B_i(q)$, and $C(q)$ have to be estimated in Equation (1), while for OE models the polynomials $B_i(q)$ and $F_i(q)$ have to be estimated. Direct identification of MIMO ARMAX and OE models is currently not possible with the system identification toolbox. Nevertheless, a MIMO state space (re)formulation of these models can be identified [Ljung, 2008]:

$$\begin{aligned} x(kT+T) &= Ax(kT) + Bu(kT) + Ke(kT) \quad (2) \\ y(kT) &= Cx(kT) + Du(kT) + e(kT) \end{aligned}$$

with parameter matrices A, B, C, D, and K. The measurements are sampled at time instants $t = kT$, with $k = 1, 2, \ldots$. To estimate the equivalent (re)formulation of an MIMO OE model, parameter K in Equation (2) is defined 0. When K is estimated too, actually a MIMO ARMAX model is created. The parameters in the general formulation (Equation (2)) are identified using the subspace identification method [Van Overschee and De Moor, 1996]. The model order for identification of the equivalent state space models is varied between 5 and 30.

To compare different models and to derive the correct model order, the Akaike Information Criterion (AIC) [Akaike, 1974, Ljung, 1999] is adopted. A lower value of AIC indicates a more accurate model. AIC is defined as:

$$AIC = \log(V) + \frac{2d}{N} \quad (3)$$

where V is the loss function, d the number of estimated parameters, and N the number of values in the estimation data set. The loss function V is equal to the determinant of the covariance matrix of the prediction error:

$$V = \det\left(\frac{1}{N}\sum_{1}^{N} \epsilon(t,\theta_N)\left(\epsilon(t,\theta_N)\right)^T\right). \quad (4)$$

The model order of the model, selected based on the minimal AIC value, is converted to its minimal realisation by pole-zero cancellation to improve numerical performance. Then, the Hankel Singular Values, representing the state energy of the different states, are determined. States with a state energies lower than 0.3 are neglected in view of an additional model reduction.

3.4 Validation

As model validation, the prediction of dataset A2 and B2 is compared with the data based on a fit measure:

$$\text{fit} = 100\%\left(1 - \frac{|\hat{y}(t) - y(t)|}{|y(t) - \bar{y}(t)|}\right) \quad (5)$$

where $\hat{y}(t)$ is the predicted output, $y(t)$ the measured output and $\bar{y}(t)$ the mean of the measured output.

To have an idea of the model accuracy, one month later, with a different ambient temperature, a new experiment has been performed. The derived models are used to predict the outputs of this new dataset. Dataset C contains the data resampled to 5 s and dataset D consists of the data resampled to 60 s. Datasets C and D are prepared in the same way as datasets A and B respectively, except that the mean value and standard deviation needed for normalisation are taken from datasets A and B.

4. RESULTS

This section describes the results for ARX and ARMAX models according to the procedure described above. Identification of OE models has resulted in inaccurate models with very high order and is therefore not discussed.

4.1 ARX model identification

The AIC index of every model is calculated and compared. For dataset A1, the model with the lowest AIC index is a model with $n_a = 9$, $n_b = 5$ and $n_k = 1$, referred to as arx951. As can be noticed in Figure 4, the AIC index is

hardly changing for varying n_a and n_b, where n_a is larger than 2. This observation allows the use of different n_a and n_b values with AIC values close to the proposed model. The reason for this flat surface can be a too fast sampling rate or in other words: new samples do not always contain new information.

State space conversion of this model results in a 70th order model. To improve numerical performance a model reduction based on pole-zero cancellation is performed, which results in a model with 49 states. The Hankel Singular Value calculation indicates that a lot of states contribute less to the dynamics of the column. So, states with a state energy lower than 0.3 will be neglected. This results in a stable model (arx951r) with 10 states. Ten zeros exists and seven are located outside the unit circle causing non-minimal phase behavour.

For dataset B1, AIC proposes a model with $n_a = 4$, $n_b = 2$ and $n_k = 1$ (arx421). This time, a clear minimum can be seen in Figure 5 for the AIC values of different ARX models. After conversion to a state space formulation and pole-zero cancellation, the original 30 states model is reduced to a 20th order state space model. Removing states with energy higher than 0.3 results in a 6th order stable model (arx421r). Six zeros exist and four of them are located outside the unit circle.

4.2 ARMAX - State Space model identification

As mentioned before, state space (re)formulations of MIMO ARMAX models are identified. In the top plot of Figure 6, the AIC values of different state space model orders for dataset A1 are depicted. As can be noticed, a minimum is reached for a model order 16 which will we referred to n4s16. For model orders increasing until 16, a steep decent is witnessed while for higher model orders only a slight increase is observed. Also this time a too fast sample rate can be the reason. Despite the shallow minimum for the AIC, a model order of 16 has been chosen to fit. A threshold of 0.3 for the state energy of the Hankel Singular Values, results in a reduced model with order 9 (n4s16r). Nine zeros exists and seven of them are located outside the inner circle, which leads to non-minimum phase behaviour.

In the bottom plot of Figure 6, a clear minimum for the AIC index for dataset B1 is reached for a model order of 13. This model is referred to as n4s13. Model reduction with Hankel Singular Value decomposition results in a 6th order model (n4s13r) with 6 poles and 6 zeros with 5 of them lie outside the unit circle.

4.3 Model validation on original data

For the identification of the models, each time the first part of every dataset has been used. For the model validation, however, the last part, i.e., dataset A2 and B2, are employed. Due to space limitations, only the resulting comparative plots of the two most important outputs are depicted. These outputs are, from the chemical point of view, the top temperature Tt and the bottom temperature Tb. A prediction horizon of 105 minutes is proposed because it takes the column approximately 90 minutes to reach steady state. For dataset A and B, these

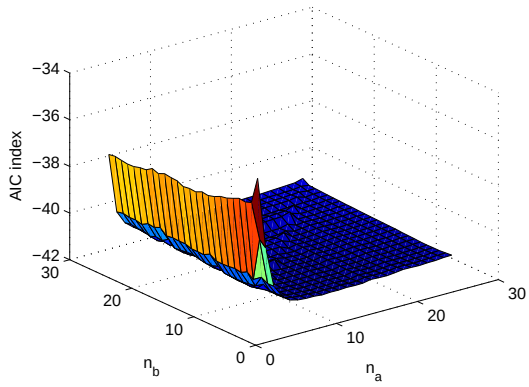

Fig. 4. Dataset A1: AIC values for ARX models with n_a and n_b varying from 1 to 25 and $n_k = 1$.

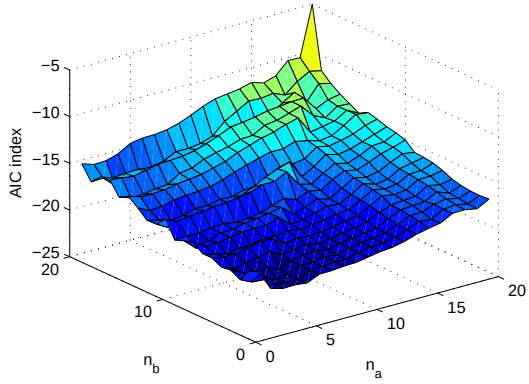

Fig. 5. Dataset B1: AIC values for ARX models with n_a and n_b vary from 1 to 20 and $n_k = 1$.

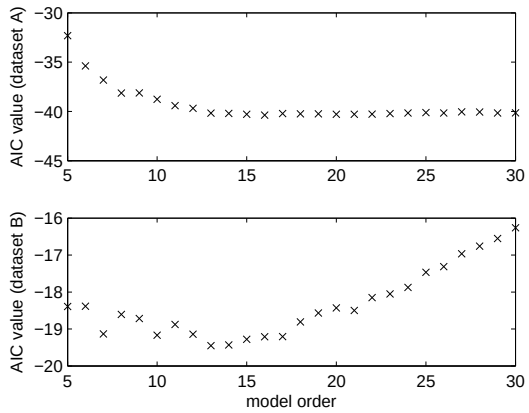

Fig. 6. AIC values for different state space model orders: Dataset A1 (top) and dataset B1 (bottom).

horizons correspond to 1260 and 105 steps respectively. On all plots, only predictions with reduced models are depicted.

For dataset A1, the general behaviour of the top temperature is predicted well as can be seen on Figure 7. However, the behaviour of the measured signal is not followed well in the peaks. The best performing reduced model is the state space model (n4s16r). This model approaches the measured signal the closest.

In Figure 8, it can be seen that the prediction for the reboiler temperature covers almost all the time the mea-

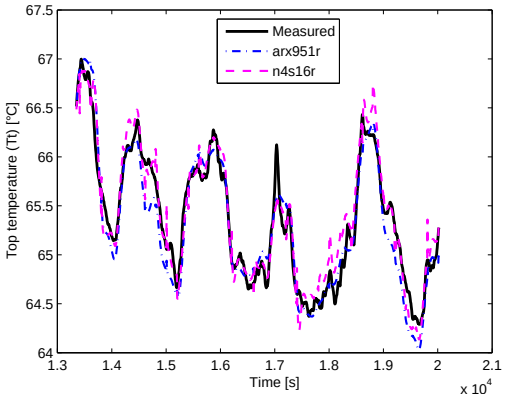

Fig. 7. Dataset A2: top temperature prediction.

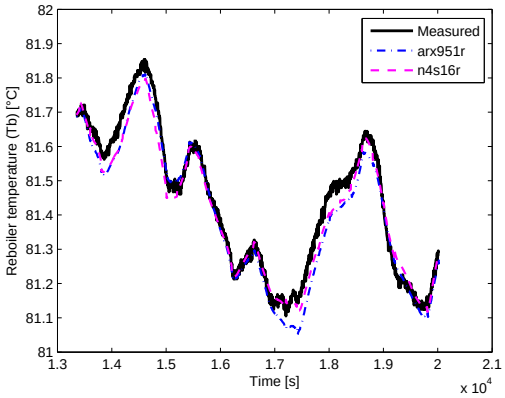

Fig. 8. Dataset A2: reboiler temperature prediction.

sured signal. The measured signal varies only 0.9 °C and becomes noisy due to normalisation. Both the ARX model (arx951) and the reduced state space model of this model (arx951r) deviate from the measured output at some peaks resulting in an offset during the second part of the prediction.

For dataset B similar conclusions can be drawn. The top temperature (see Figure 9) suffers from the same problem as in dataset A, i.e., the dynamics at the peaks are not fitted well, but the general shape is correct. The reboiler temperature (Figure 10) is predicted well but shows again an offset in the second part of the prediction.

Table 1 prints the fit values according to Equation (5). All reduced models have slightly lower fit values than the original models. Only for the reduced ARX model for dataset A (arx951) this is not the case. The higher values are caused by numerical issues, but also show there is room for further reduction. In both datasets the overall performance of the reduced ARMAX models is better than the reduced ARX models. So, these models, i.e., n4s16r and n4s13r, are the preferred model for prediction. The fit values of the corresponding models for dataset A and B are most of the time higher for dataset A. The table also shows that the best fitted temperatures is $Ts2$ or $Ts3$, followed by the reboiler temperature and the temperatures at the top of the column.

To conclude, the preferred model for both datasets is the ARMAX model in state space formulation.

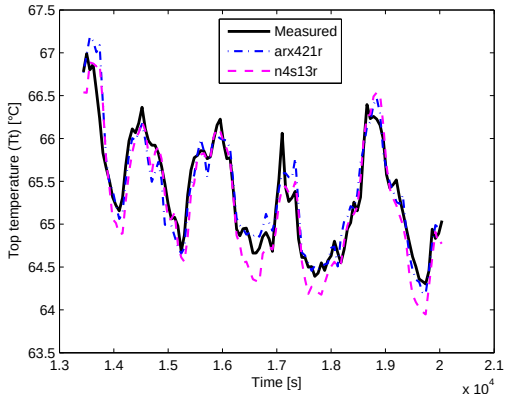

Fig. 9. Dataset B2: top temperature prediction.

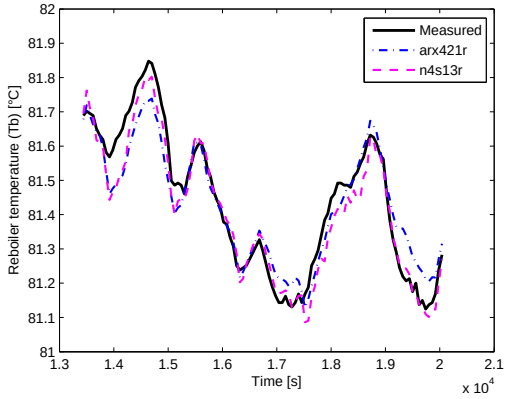

Fig. 10. Dataset B2: reboiler temperature prediction.

Table 1. Fit values for dataset A2 and B2 (%).

	Fit dataset A				Fit dataset B			
	arx951	arx951r	n4s16	n4s16r	arx421	arx421r	n3s13	n3s13r
Tt	69.5	69.6	76.0	72.3	73.4	68.0	72.4	62.4
$Ts1$	78.9	79.0	78.0	75.7	71.0	65.6	78.0	70.0
$Ts2$	85.6	85.8	85.2	81.5	79.8	72.2	82.8	76.8
$Ts3$	82.1	82.1	83.9	82.6	74.0	63.3	81.9	73.5
Tb	76.8	76.8	83.2	81.4	73.8	67.9	81.9	74.3

4.4 Model validation on new data

In priciple, the models validated in the previous subsection can be implemented. However, to have an idea of the influence of the measured and unmeasured disturbances, new data are recorded and predictions are depicted in Figures 11 to 14. These plots show a higher deviation from the measured value than the plots with the validation in the old data. Nevertheless, the general trend is still followed.

Based on the fit values presented in Table 2, the state space models still perform the best for all the temperatures, except the reboiler temperature, in both datasets. The significant deviation seen in the plots shows that not all influences are captured in the model. Possible unmeasured disturbances are the humidity and composition, i.e., the slow evaporation of the lowest boiling component out of the (closed) pilot scale column. Another step in the amelioration of the models can be taken by combining parts

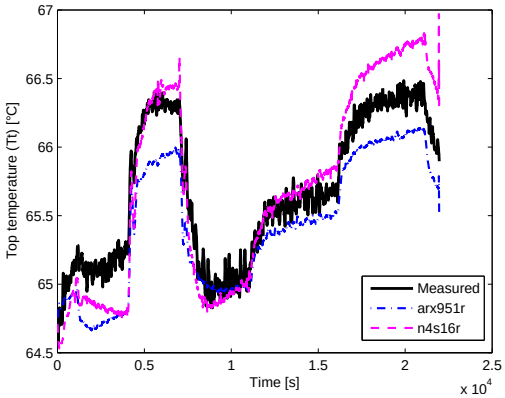

Fig. 11. Dataset C: top temperature prediction.

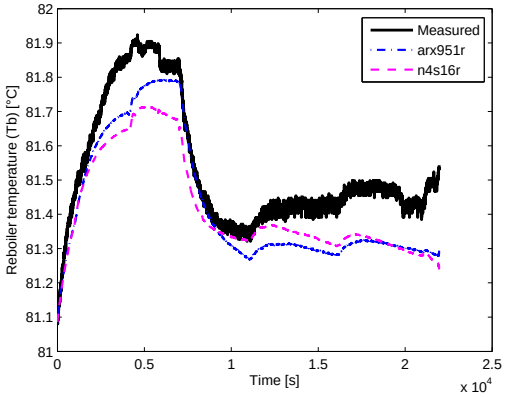

Fig. 12. Dataset C: reboiler temperature prediction.

Table 2. Fit values for dataset C and D (%).

	Fit dataset C				Fit dataset D			
	arx951	arx951r	n4s16	n4s16r	arx421	arx421r	n3s13	n3s13r
Tt	47.2	45.2	54.1	53.6	55.0	54.5	62.4	59.6
$Ts1$	21.4	21.9	34.6	33.9	19.9	17.2	24.0	18.9
$Ts2$	30.3	19.6	43.2	41.8	33.5	31.1	35.6	31.0
$Ts3$	45.2	43.5	43.4	42.8	34.8	33.2	52.9	49.1
Tb	36.3	33.5	30.8	30.4	43.2	42.0	30.9	28.2

of dataset A and C into a new set used for identification. This is currently not performed. The authors believe that an MPC controller can deal with these imperfections of the model via the repeated updates and feedback.

Currently, the ARMAX models, i.e., n4s16r and n4s13r, for sampling period of 5 s and 60 s, respectively, will be used in further work to control the temperatures of the column.

5. CONCLUSION

In this paper, two dynamic black-box MIMO models of a distillation column have been succesfully derived in view of an implementation of an MPC on PLC hardware. ARX, ARMAX and OE models have been identified and reduced to low order MIMO models in state space formulation. The best performing models, one with a sample rate of 5 s and one with a sample rate of 60 s, are both state space ARMAX models. Although not perfect, these models will be used in further research, since the authors are convinced

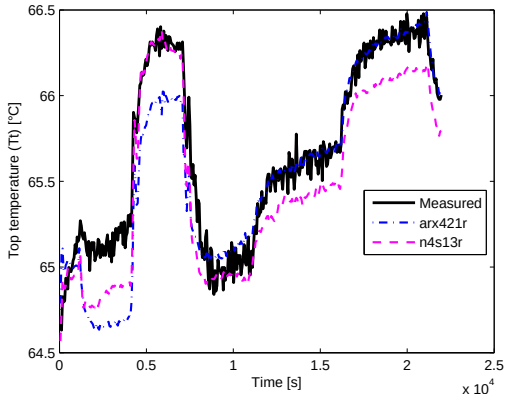

Fig. 13. Dataset D: top temperature prediction.

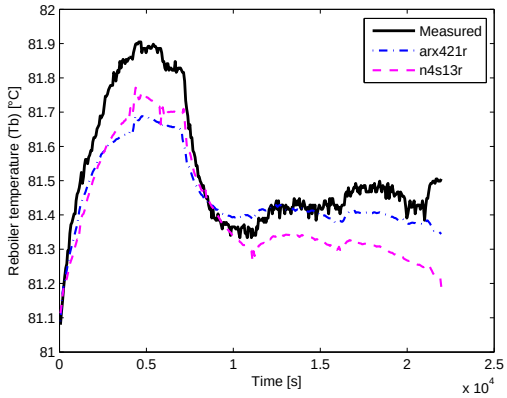

Fig. 14. Dataset D: reboiler temperature prediction.

these models are both accurate and simple enough to perform well in an MPC scheme on PLCs.

REFERENCES

H. Akaike. A new look at the statistical model identification. *IEEE Transactions on Automatic Control*, 19 (6):716–723, 1974.

L. Ljung. *System Identification Toolbox Users Guide*. The MathWorks, Inc, Natick, 2008.

L. Ljung. *System Identification: Theory for the User, Second Edition*. Prentice Hall, Upper Saddle River, New Jersey, 1999.

S. Piche, B. Sayyar-Rodsari, D. Johnson, and M. Gerules. Nonlinear model predictive control using neural networks. *IEEE Control Systems Magazine*, 3:53–62, 2000.

S. J. Qin and T. A. Badgwell. A survey of industrial model predictive control technology. *Control Engineering Practice*, 11:733–764, 2003.

P. Van Overschee and B. De Moor. *Subspace Identification of Linear Systems: Theory, Implementation, Applications*. Kluwer Academic Publishers, 1996.

ACKNOWLEDGEMENTS

Research supported by: Research Council KUL: GOA AMBioRICS, CoE EF/05/006 Optimization in Engineering(OPTEC), IOF-SCORES4CHEM, OT/03/30, several PhD/postdoc & fellow grants; Flemish Government: FWO: PhD/postdoc grants, projects G.0452.04, G.0499.04, G.0211.05, G.0226.06, G.0321.06, G.0302.07, G.0320.08, G.0558.08, G.0557.08, research communities (ICCoS, ANMMM, MLDM); IWT: PhD Grants, McKnow-E, Eureka-Flite+; Helmholtz: viCERP; Belgian Federal Science Policy Office: IUAP P6/04 (DYSCO, Dynamical systems, control and optimization, 2007-2011); EU: ERNSI; FP7-HD-MPC (Collaborative Project STREP-grantnr. 223854); Contract Research: AMINAL